Influence of the Intramedullary Stem in Total Knee Arthroplasty

Sara Beatriz Marques Freitas
sara.b.freitas@tecnico.ulisboa.pt

Instituto Superior Técnico, Lisboa, Portugal

July 2021

Abstract

Knee osteoarthritis is responsible for the progressive degradation of the knee articular cartilage. In serious cases, total knee arthroplasty is used to restore the function and alignment of the knee joint. While generally successful, complications can occur after TKA, resulting in revision surgeries. Damaged components must be removed and replaced, and intramedullary stems can be introduced, in order to increase fixation and stability. Computational models can improve the design and preoperative planning of the TKA. The main goal of this work is to analyze how the introduction of an intramedullary stem during revision surgery affects the stresses acting on the complementary bone, through finite element analysis. Therefore, four models were created, with different stem insertion configurations. Muscle forces were applied, so as to mimic the loading the prosthesis is subjected to. The main conclusion of this study is that the insertion of a tibial stem, affects insignificantly the stress distributions in the femur. Furthermore, in the cases where a femoral stem was inserted, the femur stresses lowered, thus confirming the stress shielding effect.
Keywords: Total knee arthroplasty, revision surgery, stem, Finite Element Analysis, Von Mises stress

1. Introduction

Osteoarthritis, a disease characterized by the deterioration of cartilage over time due to prolonged wear, is one of the most common chronic conditions affecting adults today. Knee osteoarthritis causes a great deal of pain to the patient, as well as directly decreasing their quality of life. When the deterioration is too severe, TKA is performed so that proper knee joint function is restored, making osteoarthritis the main indication for the procedure. Over the last decades, the total knee arthroplasty (TKA) has evolved into one of the most successful surgical procedures in modern medicine. Nevertheless, no surgical procedure is without the possibility of postoperative complications. In the case of TKA, infection and loosening of the prosthetic components are the most common sources of implant failure. In order to restore joint functionality and stability, a revision TKA may be performed, where prosthetic components are removed and replaced.

Revision TKA must deal with bone loss, inflammatory processes and stress shielding effects, and femoral and tibial components used for primary TKA may no longer provide necessary stability, on their own. As a result, revision TKA may require the use of complementary revision specific components, such as stems. Stems improve the mechanical stability of the components, by providing load transmission to diaphyseal cortical bone and away from implant interfaces [Shannon et al., 2003], at the cost of stress shielding along their length.

Modern imaging methods and CAD-software allow the reconstruction and design of biological structures, suitable for computational finite element analysis (FEA). With FEA software, joint replacement surgeries can be assessed pre-operatively, making the procedure more personalized to the specific needs of each patient.

The main goal of this study is to understand how the introduction of an intermedullary stem, during revision TKA, affects the stresses acting on the complementary bone. Four different computational models for FEA were created, representing the knee joint after primary surgery, without any stem, and three possible knee joint configurations after revision surgery, with the insertion of only a femoral or a tibial stem, or both. Comparing the four, the goal is to determine if, indeed, one stem influences the stresses on the complementary bone.

2. Background

2.1. Knee Joint Anatomy

The knee joint is the largest and most complex joint in the human body. It is comprised of two distinct joints: the tibio-femoral joint and the patella-femoral joint. The tibio-femoral joint refers to the joint formed by the proximal tibia and the distal femur. It is responsible for flexion and extension

movements of the leg, crucial for activities such as walking or running. The patella-femoral joint, formed by the patella and femur, stabilizes and protects the knee joint, with the former gliding over the latter. In addition, various stabilizers act simultaneously, in order for the knee joint to move correctly and with proper stability. The stabilization is guaranteed, primarily, by the ligaments located around the knee, while secondary stabilization is provided by the surrounding muscles. In addition, the menisci, two fibrocartilaginous discs located above each tibial condyle, act as shock absorbers. These are responsible for providing protection and increasing the stability of the knee [Affatato, 2015, Abulhasan and Grey, 2017].

The knee is stabilized by a combination of two intracapsular ligaments, the cruciate ligaments, and five extracapsular ligaments, from which the two most important are the two collateral ligaments. The anterior and posterior cruciate ligaments are two intracapsular ligaments, responsible for connecting the femur and the tibia together. The anterior cruciate ligament (ACL), attaches to the tibia anteriorly and is responsible for limiting hyperextension of the knee, while simultaneously preventing the anterior sliding of the tibia over the femur. The posterior cruciate ligament (PCL), attaches posteriorly to the tibia, limits hyperextension and prevents posterior sliding of the tibia over the femur [Derrickson and Tortora, 2017].

The lateral (or fibular) collateral ligament (LCL) prevents lateral displacement, or varus stress, of the knee. The medial (or tibial) collateral ligament (MCL) is responsible for preventing medial displacement, or valgus stress, of the knee.

The muscles acting on the knee can be divided into two groups according to their primary function: the extensors and the flexors. Muscles involved in knee extension (and hip flexion) are found on the anterior side of the knee, and include the sartorius and the quadriceps femoris. The quadriceps femoris is considered the main extensor of the knee, and is composed of four different muscles: the rectus femoris, the vastus lateralis, the vastus medialis and the vastus intermedius. All four muscles insert in the patella, via the quadriceps tendon. Distal to the patella, the quadriceps tendon extends as the patellar tendon, and inserts in the tibial tuberosity. Antagonistic to these are the hamstring muscles, responsible for knee flexion (and hip extension). These are three different muscles, the bicep femoris, the semimembranosus and the semitendinosus [Van Putte et al., 2016].

2.2. Total Knee Arthroplasty

As previously mentioned, TKA is recommended for cases where the knee joint is severely damaged by diseases such as osteoarthritis or rheumatoid arthritis, or by a traumatic knee injury or deformity. In severe cases, chronic pain is debilitating to the patient, leading to a significant decrease in quality of life. Therefore, the main goal of a TKA is to restore joint stability and relieve pain [Affatato, 2015].

When performing a TKA, the surgeon must choose between different categories of prosthesis, namely unconstrained, semiconstrained and constrained. The type to be used is decided according to the underlying condition of the patient, the degree of articular damage present and the age of the patient. A semiconstrained prosthesis is recommended for superficial replacement of the joint. When the PCL is sacrificed, a posterior stabilized implant can be used [Tateishi, 2001]. The use of posterior stabilized design for TKA is becoming increasingly popular as its benefits include easier balancing of varus/valgus deformities and greater posterior femoral rollback. Furthermore, it is possible that it may also result in less component wear and greater flexion range [Indelli et al., 2014].

In this study, the knee prosthesis referenced is the SIGMA® Posterior Stabilized (PS) Fixed Bearing Knee System. It is comprised of 3 main components, a femoral component, a tibial tray and a tibial insert. For revision surgeries, stems are added as a way of enhancing the stability of the knee joint. The stems considered in this study are the SIGMA® Universal Press-Fit Stems, with 14mm diameter. The femoral stem used is 125mm long, at 7° valgus, while the tibial stem is 75mm [DePuy, 2017].

3. Implementation

Numerical models were created in order to study the biomechanical behaviour of the prosthetic knee joint. To create these models, medical images of the knee joint were put through a segmentation process. Then, CAD and FEA software were used to build the models and assign the necessary properties for the simulation.

3.1. Image Acquisition, Bone Segmentation and Computacional Modelling

CT images of a female left knee were used for the bone segmentation process, performed through ITK-SNAP [Ribeiro et al., 2009]. The results were filtered in MeshLab (version 1.3.4BETA) and imported into SolidWorks® (version SP02, 2019). Using the ScanTo3D® toolbox, two surface bodies were created, to act as a base for the 3D solid bone models, created with the use of the Loft surface tool. In order to obtain distinct cortical and trabecular bone regions, trabecular bone portions of the femur and tibia were created as solid bodies, positioned inside the full solid bone models. The cortical bone regions are created later on, in ABAQUS®. As for

the geometric modelling of the prosthesis, the computational 3D models of the components used had already been obtained in a previous work [Moreira, 2018].

3.2. Assembly Process

The assembly process was then performed. In order to study the primary surgery case, one of the 3D models was assembled without any stems. As for the revision surgery, all possibilities had to be studied. Thus, 3 models were created, one with a tibial stem, one with a femoral stem, and one with both. All models included the fibula, although not yet attached to any other bone. The connections between the fibula and the femur and tibia, assured by the LCL and the Posterior Tibiofibular Ligament (PTL), respectively, are performed later on in ABAQUS®. Once the final 3D computational models were obtained, shown in Figure 1, they were exported as Parasolid format files to ABAQUS® (2020 version), a software suited for finite element analysis.

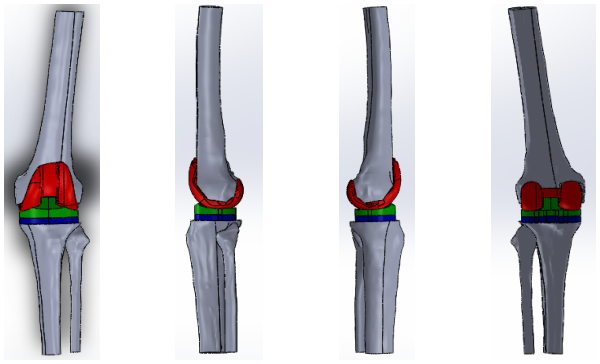

(a) (b) (c) (d)

Figure 1: Anterior (a), Lateral (b), Medial (c) and Posterior views of the 3D computational model of the knee joint with insertion of the SIGMA® Fixed Bearing knee prosthesis, Cortical and trabecular bone displayed on SolidWorks®.

3.3. Numerical Modelling

Once the numerical models were imported into ABAQUS®, the cortical bone portions were created, resorting to the Cut tool, which was used to create a cavity in the full bone solid bodies, coincident with the trabecular bone. Ensuing, the cortical and trabecular bone models were merged, creating a single bone part with distinct cortical and trabecular portions.

FE models of the LCL and MCL were created with a wire shape and tenson-only truss sections and assembled to the complete knee joint FE model. The ligaments were also modelled with a 2% prestretch [Liacouras and Wayne, 2007]. Notably, a simplified version of the combined anterior and posterior proximal tibiofibular ligament (PTL), responsible for connecting the tibia and fibula, was modelled. Three springs, with a stiffness of k=10^6N/m were created, in order to model the PTL. Each spring was modelled to prevent displacement in each of the three translational degrees of freedom. All ligaments were connected to the bone models by Coupling interactions, with attachment surfaces being defined for each ligament insertion point.

3.3.1 Mechanical Properties of the Materials

Bone was defined as a linear elastic, isotropic and homogeneous material, with different Young's Modulus (E, in MPa) values selected for the cortical and trabecular bone. Each material of the prosthetic components was defined as linear, elastic and isotropic, as well. All the material properties and parameters assigned to each part of the model (including the femoral and tibial stems), are presented in Table 1.

3.3.2 Contact and Boundary Conditions

Ensuing, the interactions and constrains between the different elements of the assembly were defined. A Tie constraint was used, between the tibial tray inferior surface and the resected tibial surface. As for the femoral component, a surface-to-surface contact with cohesive behaviour properties was chosen. A Tie constraint was also used to bond the tibial polyethylene insert and the tibial tray, as the two components are designed with a locking mechanism, as previously mentioned.

For the tibial keel- tibia contact, as well as the stem-tibia and stem-femur contacts a surface-to-surface contact with a coefficient of friction of 0.3 was used [Viceconti et al., 2000, Robalo, 2011]. In addition, both the distal tibial and fibular ends were pinned with the boundary condition "Encastre".

Furthermore, since the femoral component and tibial insert were not connected, it was necessary to constrain the FE model so that the numerical model could converge. Thus, six springs with a stiffness of k=10^6N/m, were added to the model with the goal of constraining movement in all six degrees of motion (3 translational and 3 rotational). Each spring was connected to two overlapping reference points, one coupled with the femoral component surface and the other coupled with the tibial insert surface. Both Coupling interactions were modelled with continuum distribution and uniform weighting.

3.3.3 Load Conditions

In order to recreate as closely as possible the loading that a real knee is subjected to, two groups of forces were applied to the FE model, the joint reaction forces and the muscle tendon forces.

Firstly, the joint reaction forces were obtained

Table 1: Material type and the corresponding properties and parameters (Young's Modulus and Poisson's Ratio, attributed to the final FE model of the knee joint, prosthetic components and stems).

	Model Part	Material Type	Material Property	Young's Modulus E (MPa)	Poisson's Ratio ν	References
Bones	Femur	Cortical Bone		17000	0.3	[Heiner, 2008]
		Trabecular Bone		1000		[Ryan and Williams, 1989]
	Tibia	Cortical Bone	Elastic, Isotropic and	17000		[Heiner, 2008]
		Trabecular Bone	Homogeneous	1000		[Ryan and Williams, 1989]
	Fibula	Cortical Bone		17000		[Heiner, 2008]
Ligaments	LCL	Ligament	Elastic and Isotropic	493.86	0.4	[Cho and Kwak, 2020],
	MCL			326.75	0.4	[Orozco et al., 2018]
Prosthesis	Femoral Component	Co-Cr Alloy		210000	0.36	[Eidel et al., 2020]
	Tibial Insert	XLK Polyethylene	Elastic and Isotropic	900	0.46	[Kang et al., 2019]
	Tibial Tray	Co-Cr Alloy		210000	0.36	[Eidel et al., 2020]
	Femoral Stem	Titanium	Elastic and Isotropic	110000	0.33	[Eidel et al., 2020]
	Tibial Stem	(Ti-6AI-4V Alloy)				

from the free public data base, OrthoLoad. These forces are measured through the use of instrumented implants and are based on the study by [Kutzner et al., 2010], where forces and moments acting on the tibial component during daily living activities are measured *in vivo*. For this study, six loading cases corresponding to six instances of the walking gait cycle were considered. Since the forces were measured on a 100kg male's right knee, conversations were made to fit a 70kg female's left knee. Furthermore, since the model in this study contains not only a tibia, but also a femur, the application point for these reaction forces and moments was altered, to a reference point coupled to the uppermost surface of the femur. Considering the model to be at static equilibrium, the forces applied at the center of the tibial component remain the same at the femur surface. However, the new moment values must account for the distance to the center of the tibial component. Thus, a vectorial product was used to determine the new moment values, resulting in the following equation system 1.

$$\begin{cases} M_x^{'} = M_x + F_z d_y - F_y d_z \\ M_y^{'} = M_y + F_x d_z - F_z d_x \\ M_z^{'} = M_z - F_x d_y + F_y d_x \end{cases} . \quad (1)$$

As for the muscle forces, four muscles were considered: the bicep femoris (BF), the semimembranosus (SM), the TRIPOD (a combination of the sartorius, gracilis and semitendinosus muscles), as well as the distal portion of the quadriceps femoris tendon, known as the patellar tendon (PT). Insertion sites were modelled as reference points, coupled to the tibial anterior and posterior surfaces, with locations defined according to anatomical images. In a work by Adouni, muscle tendon forces were computed at six instances of the walking gait cycle, between 0% (heel strike phase) and 100% (preswing phase) [Adouni et al., 2012]. These six instances correspond to the instances considered for the joint reaction forces. In order to compute the forces, the orientation of the muscle tendons ([Aalbersberg et al., 2005]) and the ratio to body weight values ([Adouni et al., 2012]) were considered.

3.3.4 FE Mesh Generation

Finally, each part of the FE model was meshed. Linear Tetrahedral elements were used for all model parts, with an element size of 2mm considered for the femur and tibia. As for the remaining components, as they are not the focus of this study, larger element sizes were chosen to minimize computacional cost, in specific to minimize the duration of each simulation, as these could take between 20 and 30 minutes each. A representantion of the final FE mesh used on the models is shown in Figure 2. Notably, when meshing the LCL and MCL, only one element per ligament was considered. Therefore, each ligament only presented two nodes.

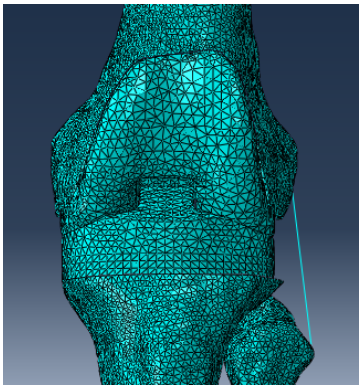

Figure 2: Mesh applied to the final FE knee joint model.

4. Results and Discussion

As previously mentioned, the goal of this study is to assess how the insertion of an intramedullary stem

influences the stresses of the complementary bone. As a simplication, the models will be referred to as Reference Model, Tibial Stem Model, Femoral Stem Model and Both Stems Model, according to their stem configuration. As this study is focused on the stem insertion effects on the femur, result comparisons will be focused on the Reference, Tibial Stem and Both Stems models.

Finite element analysis was performed on each of the models, and biomechanical comparisons were made in order to confirm the hypothesis previously mentioned. In a previous work, Completo thoroughly analyzed how femoral stems influenced the tibia and vice-versa, in terms of stress and stability. As expected, it was concluded that stress-shielding, which is the reduction in bone density as a result of removal of stress from a bone by an implant, occurred on the femur whenever a femoral stem was used, and that the inclusion of a tibial stem did not noticeably affect the stability of the femoral component, or of the bone/cement interface. As for the strain displayed by the femur, the changes resulting of the tibial stem insertion were considered insignificant [Completo, 2006].

4.1. Analysis of the Stress-Shielding Effect

A macroscopical analysis of the Von Mises stress distribution on the femur was performed, in order to confirm the stress-shielding effect resultant of the femoral stem insertion, as well as the impact of the tibial stem insertion.

Firstly, the stress shielding effect is addressed. According to Hooke's Law, stress is linearly dependent on a material's stiffness, or Young's Modulus, as described in Equation 2.

$$\sigma = E * \varepsilon \tag{2}$$

Since cortical bone presents a much higher Young's Modulus than trabecular bone, it is expected that larger stress values are found on the former. The results obtained confirm that the greatest values of Von Mises stress are found along the cortical section of the diaphysis, where the cortical bone thickness is greater. In contrast, the trabecular bone presents very small Von Mises stress values, confirming that the majority of the stress is supported by the cortical bone. When a femoral stem is included, as in the Both Stems model, as shown in Figure 3, there is a decrease in the Von Mises stress on the cortical bone. It is particularly noticeable closest to the femoral distal epiphysis, where in some regions, the stress seems to decrease in half, when compared to the Reference Model.

4.2. Analysis of the Von Mises Stress Distribution

Ensuing, the insertion of a tibial stem in the model was studied, again observing the femoral Von Mises stress variation. Thus, side by side comparisons of the femoral stress values were made, between the Reference, Tibial Stem, Femoral Stem and Both Stems models. All six instances of the walking gait cycle were analyzed, in order to compare the stem influence during normal activity, in a similar fashion to the example shown in Figur 4. Comparing the four models, it is possible to see a decrease on the Von Mises Stress on the cortical surface. This is particularly noticeable on the distal epiphysis region.

Comparing the Reference and Tibial Stem models, the models are a quite similar Von Mises distribution, with the changes observed macroscopically being almost none. Hence, it is possible to conclude that, on this study, no significant impact on the stress distribution on the femur was observed macroscopically, as a result of a tibial stem insertion alone.

As for the models with femoral stem insertion, the Von Mises stress values decrease consistently on all six instances of the walking gait, when compared to the Reference and Tibial Stem models. Also, on both models, the decrease is very similar, although slightly more significant in the Both Stems Model. This decrease can, again, be attributed to the stress-shielding effect caused by the insertion of the femoral intramedullary stem. The similarity between the two model proves that, much like in the previous comparison, the tibial stem influence is insignificant on the femoral stress values. While this type of analysis is enough to confirm if a decrease in the Von Mises values occurs or not, it can not quantify how significant that change is. In order to do so, a nodal analysis where the stress values of specific nodes are compared, can be used.

4.3. Nodal Analysis of the FE models

Four nodes, highlighted and shown in Figure 5, on different location of the femoral surface were carefully chosen to be analyzed. For the different models, the Von Mises stress values of these four nodes were obtained and compared. Again, all stance phases were considered.

An average of the reference points' Von Mises values for each walking gait instance, of each model, was calculated, as well as an average of the stress values measured for each reference point. In order to compare the results for each model, and to quantify how much the stress values decreased, the relative standard deviation (RSD) between the nodal stress values of the Both Stems model and the nodal stress values of the Reference model, as well as between the nodal stress values of the Both Stems model and the nodal stress values of the Tibial Stem model was calculated, according to equation 3 and 4, respectively. All results are included in Tables 2

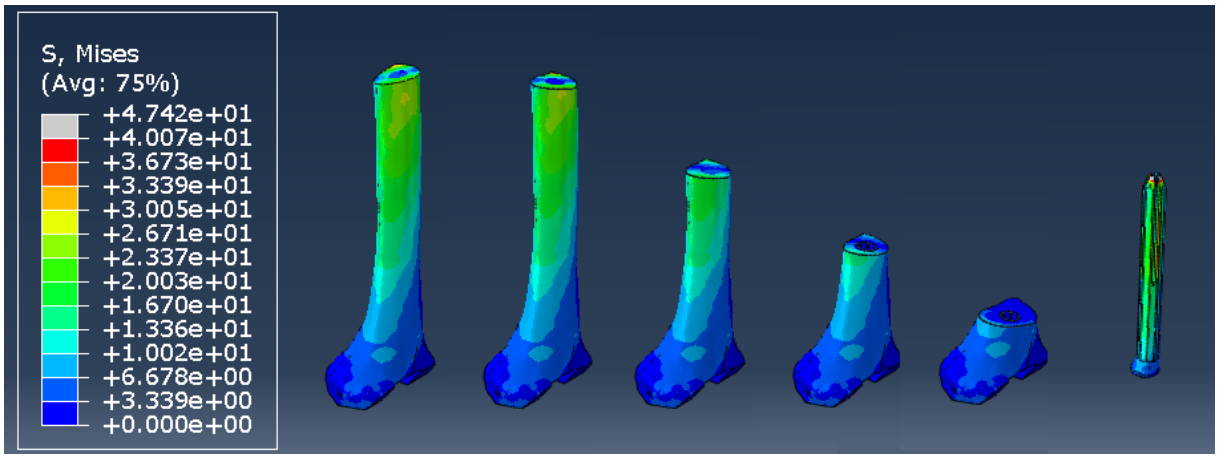

Figure 3: Von Mises Stress Distribution (in MPa) for Axial Cuts of the Both Stems Model femur, at 75% stance phase

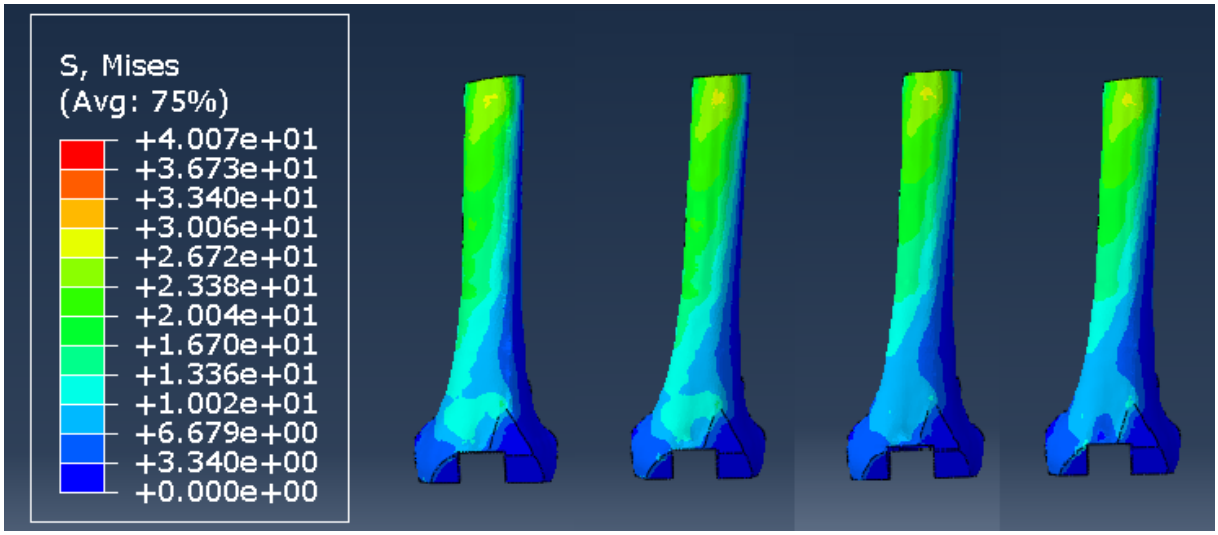

Figure 4: Comparison of the femoral Von Mises stress distribution of the Reference, Tibial Stem, Femoral Stem and Both Stems models, at 75% Stance Phase..

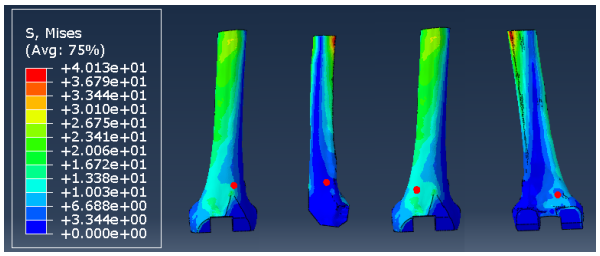

Figure 5: Highlighted representation (red dots) of the femoral surface nodes (1 to 4) chosen for analysis.

and 3.

$$RSD\ (Both\ Stems\text{-}Reference) = \frac{\sigma_{bs} - \sigma_r}{\sigma_r} * 100 \quad (3)$$

$$RSD\ (Both\ Stems\text{-}Tibial\ Stem) = \frac{\sigma_{bs} - \sigma_{ts}}{\sigma_{ts}} * 100 \quad (4)$$

In Table 2, the average Von Mises stress between the four nodes analyzed, for each gait cycle instant considered is presented. Firstly, a comparison of the values between different instances with the results obtained in Subsection 4.2 is made. The results are consistent, as the highest stress values are obtained in the same instances as in the previous subsection. Comparing the values obtained between models, the Reference Model and the Tibial Stem Model present very similar average values, with residual relative standard deviations, all below 4%. Therefore, it is safe to conclude that the tibial stem insertion did not affect the Von Mises stress values of the selected nodes.

Table 2: Average Von Mises stress values between the four reference points, for each stance phase percentage, of each model. Relative Deviation between the average Von Mises stress values calculated for the Both Stems model, and the Reference and Tibial Stem models.

	Average Von Mises Stress (MPa)				RSD of the BS Model (%)	
Stance Phase	Reference	Tibial Stem	Femoral Stem	Both Stems	Reference	Tibial Stem
0	2.24	2.22	1.82	1.78	-21	-19.7
5	2.66	2.64	1.81	2.33	-13	-11.8
25	5.49	5.37	4.29	4.17	-24	-22.3
50	4.42	4.28	3.56	3.47	-21	-18.8
75	6.27	6.14	4.89	4.77	-24	-22.3
100	1.85	1.82	1.54	1.51	-18	-16.9

Table 3: Average Von Mises stress values of all stance phase percentage considered, for each reference point. Relative Deviation between the average Von Mises stress values calculated for the Both Stems model, and the Reference and Tibial Stem models.

	Average Von Mises Stress (MPa)				RSD of the BS Model (%)	
Ref Point	Reference	Tibial Stem	Femoral Stem	Both Stems	Reference	Tibial Stem
1	4.26	4.15	3.26	3.35	-21	-19.4
2	2.24	2.24	1.67	2.01	-10	-10
3	5.20	5.18	4.19	3.89	-25	-24.9
4	3.59	3.40	2.80	2.78	-23	-18.3

As for the Both Stems Models, in all the instances considered, the nodal stress values decreased, in comparison with the other two models. In terms of relative deviation results, when comparing the Both Stems model and the Reference Model, the average decreases between 13% and 24%. For the Tibial Stem model comparison, the deviation is quite similar, with decreases between 11% and 23%.

Moreover, the results obtained when considering for each reference point, shown in Table 3, the average between all six instances, are coherent with the results obtained thus far. The results obtained for the Reference and Tibial Stem models are, again, quite similar, with very small deviations. The deviations between the Both Stems and the Reference model are between 10% and 25%, as are the deviations between the Both Stems and the Tibial Stem model. Similarly to before, these results indicate a relation between the insertion of the femoral stem with a decrease in stress values in the femur, while the tibial stem insertion does not have a significant effect on them.

4.4. Influence of changes in the Trabecular Bone Stiffness on the Nodal Von Mises Stress Values

Different Young's Modulus values were attributed to the trabecular bone, so as to confirm the results previously obtained, by determining whether the stresses were being correctly distributed to the cortical bone. Since the intermedullary stems are in contact not only with cortical bone, but also with trabecular bone, an incorrect transfer of the stresses to the trabecular bone could occur, due to its much lower Young's Modulus. The models were analyzed with two different trabecular E values.

Firstly, a trabecular bone Young's Modulus of $E = 3$GPa was considered. The Von Mises nodal stress values were calculated for the same nodes referenced in Section 4.3. Additionally, the average values for each instance and for each node, and the relative standard deviations between models were calculated as well. Comparing the results of these models, with the results previously obtained in Section 4.3, the average Von Mises stress values of the cortical surface nodes, decrease when the trabecular bone is considered at 3GPa. This means that, considering a stiffer trabecular bone, it will support greater stress values, transferring less to the cortical bone surface.

As for the relative deviations, in all cases there is a decrease in the stress values for the Both Stems Model, when compared to the Reference and Tibial Stem models. When compared with the Reference model, the stress decrease percentage is between 15 and 29%, for the average for each instance, and it is between 4 and 37%, when comparing the average

for each reference point. As for the Tibial Stem model comparison, the relative deviation is similar, between 14% and 28%, and between 4% and 35%, for each case, respectively.

Secondly, a Young's Modulus of $E = 17$GPa was considered, in order to study how the results would be affected, considering a uniform bone stiffness for the entire bone. The stress averages decreased as well, for all the cases considered. Hence, the trabecular bone supports an even greater amount of stress, as it was expected. Again, the nodal stresses measured for the Both Stems model are lower than the ones measured for the Reference model, decreasing between 2 and 33%, for the averages of each instance, and between 0 and 41%, for the averages of each reference point. Similar results were obtained in comparison with the Tibial Stem model, with respective decreases between 1.4 and 33%, and between 0 and 40%. After analyzing the models with different trabecular bone stiffness values, and comparing them to the original model, with a Young's Modulus of $E = 1$GPa, it is possible to conclude that cortical surface stress is inversely proportional to trabecular bone stiffness. This results from the fact that a stiffer trabecular bone will absorb greater amounts of stress, as expected through Hooke's Law. As for the comparisons between different models, stem configuration wise, the relative deviations remained similar for the different E values considered. Thus, the model studied with trabecular bone stiffness $E = 1$GPa, can be considered adequate for the study of Von Mises stress distribution to the cortical surface.

5. Conclusions

The main goal of this work was to assess whether a stem insertion, typically used for revision TKAs, influences the stresses on the complementary bone. For that, finite element analysis was used and four different knee joint models were created, representing a primary surgery case, and three different possible revision surgery configurations.

In order to create these models, CT images of a knee were used as a basis for the creation of the bone models, while the prosthetic components were modelled based on scannings of real components. The model was assembled using a CAD software program, and in the finite element analysis software, the mechanical properties of the materials of each component, the interactions and contacts, the loading conditions and the mesh were defined.

Firstly, the Von Mises stress distribution was analyzed on a macroscopical level for each of the model configurations. Firstly, this analysis was used to confirm the stress-shielding effect on the femur as a result of a femoral stem insertion. Secondly, femoral stress distributions of the four models were compared side by side, to detect variations from the reference model. In this, the insertion of a tibial stem was determined to not affect in a significant manner, the stress distribution, when compared to the reference model.

Then, a nodal analysis was performed, in which four nodes of the femoral mesh were chosen and their Von Mises stress values were collected, and compared between models. In order to easily compare the data, two different methods were used. Firstly, the average value of the four nodes was measured, for each instance, and for each model. Secondly, the average of the six instances considered was measured, for each reference point, and for each model. Furthermore, the relative standard deviations between the Both Stems model and the Reference Model, and between the Both Stems model and the Tibial Stem model, were determined. Again, no significant differences were obtained, as a result of the tibial stem insertion. As for the femoral stem influence, a stress value decrease between 10 and 25% was registered for each case considered.

Finally, different Young's Modulus values for the trabecular bone were tested, namely E was altered to 3GPa and 17GPa. When comparing with the results of the initial value of 1GPa, all results were consistent. The tibial stem insertion did not produce significant impact in the Von Mises nodal stress values, and the femoral stem insertion caused a decrease in the femoral stress values, due to the stress shielding effect.

After analysing the results, one can conclude that the insertion of a tibial stem does not significantly affect the stress distribution on the femur, for both a macroscopical analysis of the Von Mises stress distribution, and a nodal analysis of various nodal points on the femoral surface. However, when a femoral stem is introduced, the Von Mises stress magnitude on the femur decreases, as expected, thus confirming the stress shielding effect resultant of the insertion of a titanium stem. These results are aligned with the work of Completo, who determined that, although the use of a tibial stem can decrease the femur/femoral component interface stability, the effects on the femoral strain are insignificant [Completo, 2006].

6. Short-comings, Improvements and Future Work

The examples discussed in this section correspond to limitations of the study developed, and can also be considered as suggestions of issues to keep in mind, in future works exploring the same topic.

Firstly, the bones went through a simplification process during the geometrical modelling phase. After the segmentation process, previous works imported the files to a CAD software and the modelling of the bones was performed according to these results. In this particular study, the bones were

modelled as approximated solid bodies, in order to simplify the meshing of these parts. Due to this, an accurate distribution of the bone density values was sacrificed, as it was no longer possible to use the information of the CT images to transform Hounsfield Unit values into apparent density values. Thus, the bones were divided into linear, isotropic and homogeneous portions of cortical and trabecular bone, with Young's Modulus values of 17GPa and 1GPa, respectively.

Evidently, this simplified model does not accurately reflect the stress distribution on the bones, with or without stems included, as stress values are directly correlated with the value of the Young's modulus, according to Hooke's Law. Therefore, most certainly, the stress values obtained are not as accurate as they would be if the bone density values were calculated from the CT image information.

Secondly, when creating the simplified bone models, the trabecular portion was modelled by offsetting the full solid body bone model. When performing these offsets, the theoretical cortical thickness of the bones was followed as much as possible. Theoretically, the stem is introduced inside the intermedullary canal, and its tip will, at some point, contact cortical bone and become completely surrounded by it. Nevertheless, it is virtually impossible to represent this interaction absolutely perfectly. Since an approximation was considered, it was not possible to recreate this ideal scenario. The stem tips do contact cortical bone, but they do so intermittently with trabecular bone. It is possible that, due to this contact with the trabecular bone, with a much lower stiffness, the stem was not able to support the correct load it would have in an ideal situation. Therefore, the stress values on the cortical surface of the femur could have possibly decreased even more, had the stem tip been completely in contact with cortical bone.

Furthermore, when performing nodal analysis, nodes from each model's mesh are considered. Evidently, stem insertion alters the bone parts, resulting in different meshes being applied. Thus, some of the nodes considered, not all, presented slight coordinate differences between models. As a result, the difference between stress values obtained may have been influenced by these differences.

Finally, due to meshing limitations, only nodes on the femoral surface were available to analyze. If it had been possible, analyzing the Von Mises stress of interior points on the femur, closer to the intermedullary canal and the stem would have been of interest for this type of work.

7. Acknowledgement

This document was written and made publically available as an institutional academic requirement and as a part of the evaluation of the MSc thesis in Biomedical Engineering of the author at Instituto Superior Técnico. The work described herein was performed at the Department of Mechanical Engineering (DEM) of Instituto Superior Técnico (Lisbon, Portugal), during the period September 2020-July 2021, under the supervision of Prof. João Folgado, Prof. Luís Sousa and Dr. Mário Gamelas.

References

S. Aalbersberg, I. Kingma, J. L. Ronsky, R. Frayne, and J. H. Van Dieën. Orientation of tendons in vivo with active and passive knee muscles. *J Biomech*, 38(9):1780–1788, 2005. DOI: 10.1016/j.jbiomech.2004.09.003.

J. F. Abulhasan and M. J. Grey. Anatomy and physiology of knee stability. *J Funct Morphol Kinesiol*, 2(34), September 2017. DOI: 10.3390/jfmk2040034.

M. Adouni, A. Shirazi-Adl, and R. Shirazi. Computational biodynamics of human knee joint in gait: From muscle forces to cartilage stresses. *J Biomech*, 45(12):2149–2156, 2012. DOI: 10.1016/j.jbiomech.2012.05.040.

S. Affatato. *Surgical Techniques in Total Knee Arthroplasty (TKA) and Alternative Procedures.* 2015. ISBN 9781782420385.

H. J. Cho and D. S. Kwak. Mechanical properties and characteristics of the anterolateral and collateral ligaments of the knee. *Applied Sciences*, 10(18), 2020. DOI: 10.3390/app10186266.

A. Completo. *Estudo Numérico e Experimental da Biomecânica da Prótese do Joelho.* PhD thesis, Universidade de Aveiro, Departamento de Engenharia Mecânica, 2006.

DePuy. Sigma: Knee Revision Reference Cards, 2017.

B. H. Derrickson and G. J. Tortora. *Principles of anatomy and physiology.* John Wiley Sons, Inc., 15th edition, 2017. ISBN: 978-1-119-41482-7.

B. Eidel, A. Gote, C. P. Fritzenb, A. Ohrndorf, and H. J. Christ. Tibial implant fixation in tka worth a revision? – how to avoid stress-shielding even for stiff metallic implants. *Computer Methods in Biomechanics and Biomedical Engineering*, September 2020. DOI: 10.1080/10255842.2020.1830274.

A. D. Heiner. Structural properties of fourth-generation composite femurs and tibias. *J*

Biomech, 41:3282–4, August 2008. DOI: 10.1016/j.jbiomech.2008.08.013.

P. Indelli, M. Marcucci, A. Graceffa, S. Charlton, and L. Latella. Primary posterior stabilized total knee arthroplasty: analysis of different instrumentation. *J Orthop Surg Res*, 9(54), 2014. DOI: 10.1186/s13018-014-0054-y.

K. Kang, T. Tien, M. C. Lee, K.-Y. Lee, B. Kim, and D. Lim. Suitability of metal block augmentation for large uncontained bone defect in revision total knee arthroplasty (tka). *Journal of Clinical Medicine*, 8:384, March 2019. DOI: 10.3390/jcm8030384.

I. Kutzner, B. Heinlein, F. Graichen, A. Bender, A. Rohlmann, A. Halder, A. Beier, and G. Bergmann. Loading of the knee joint during activities of daily living measured in vivo in five subjects. *Journal of Biomechanics*, 43:2164–2172, 2010. DOI: 10.1016/j.jbiomech.2010.03.046.

P. C. Liacouras and J. S. Wayne. Computational modeling to predict mechanical function of joints: Application to the lower leg with simulation of two cadaver studies. *J Biomech Eng*, 129(6):811, 2007. DOI: 10.1115/1.2800763.

M. C. Moreira. Analysis of the bone stresses for a posterior stabilized knee prosthesis with an endomedullary stem. Master's thesis, Instituto Superior Técnico, 2018.

G. A. Orozco, P. Tanska, M. E. Mononen, K. S. Halonen, and R. K. Korhonen. The effect of constitutive representations and structural constituents of ligaments on knee joint mechanics. *Scientific Reports*, 8(1), 2018. DOI: 10.1038/s41598-018-20739-w.

N. S. Ribeiro, P. C. Fernandes, D. S. Lopes, J. O. Folgado, and P. R. Fernandes. 3-D solid and finite element modeling of biomechanical structures - a software pipeline. *7th EUROMECH Solid Mechanics Conference*, 1 2009.

T. J. Robalo. Analysis of bone remodeling in the tibia after total knee prosthesis. Master's thesis, Instituto Superior Técnico, 2011.

J. C. Ryan and J. L. Williams. Tensile testing of rodlike trabeculae excised from bovine femoral bone. *J Biomech*, 22(4):351–5, 1989. DOI: 10.1016/0021-9290(89)90049-3.

B. D. Shannon, J. F. Klassen, J. A. Rand, D. J. Berry, and R. T. Trousdale. Revision total knee arthroplasty with cemented components and uncemented intramedullary stems. *The Journal of Arthroplasty*, 18(7):27–32, 2003. DOI: 10.1054/S0883-5403(03)00301-2.

H. Tateishi. Indications for total knee arthroplasty and choice of prosthesis. *JMAJ*, 44(4):153–158, 2001.

C. Van Putte, J. Regan, and A. Russo. *Seeley's Essentials of Anatomy and Physiology*. McGraw-Hill Education, 9th edition, 2016. ISBN: 9780078097324.

M. Viceconti, R. Muccini, M. Bernakiewicz, M. Baleani, and L. Cristofolini. Large-sliding contact elements accurately predict levels of bone-implant micromotion relevant to osseointegration. *Journal of Biomechanics*, 33:1611–1618, 2000. DOI: 10.1016/s0021-9290(00)00140-8.